TECHNISCHE MECHANIK, 32, 6, (2012), 698 – 713
submitted: January 26, 2012

Stress Waves in a Stamping Tool: Analytic Treatment of a One-dimensional Model

C. Schwarz, E. Werner, H. J. Dirschmid

A simple one-dimensional model for a stamping process is set up, taking into account the compliance of the workpiece. Two kinds of boundary conditions are considered at the end where the impact takes place. The one dimensional wave equation, describing the displacement of the cross-sections of the tool with non-trivial boundary conditions is solved by means of the Laplace transformation. The technique used for the inverse transformation back into the time domain allows for a closed-form representation and efficient numerical evaluation of the solution. The result is finally discussed with regard to the influence of the compliance of the workpiece on the loading of the tool. Restricting the discussion to a special limit case, we can show that the results agree with those found in the literature.

1 Introduction

The purpose of this contribution is to present the closed-form analytical solution for the dynamical loading of the tool in a simple model for a stamping process. Rather than addressing mechanical minutiae of the process, the focus lies on the detailed presentation of an elegant and exact solution technique to the one-dimensional problem of wave-propagation in the stamping tool. The latter is modelled as a rod which is mounted to a spring that represents the workpiece, see also Schwarz et al. (2010a). The concept for this technique has only recently been roughly sketched in Schwarz et al. (2010b).
The idea for the treatment of the stamping problem was developed from a topic discussed earlier in the context of a possible application of ceramic valves in engines, see Werner and Fischer (1995). Similar problems have already been treated and were analytically solved in the literature, see for example Zharkova and Nikitin (2006); YuFeng and DeChao (1998), however not in the generality considered here and with different emphasis.
The maximal loading of a valve or a stamping tool due to the impact on the valve seat or on the workpiece is determined by the compliance of the particular counterpart. The delicate deviation of the stress responses for a spring and for a rigid counterpart requires an unimpeachable solution technique leaving no space for ascribing the observed effects to numerical inaccuracies.
In a one-dimensional consideration, both applications can be described by the rod-spring-model with adequate initial and boundary conditions. The valve is initially moving and actually impacts on the seat by itself, whereby the opposite end remains stress-free. The stamping tool is modelled to be initially at rest and in contact with the workpiece when either (a) a mass impacts or (b) a force is applied for a finite time t_{F} at the opposite end. In a simplified way, that is neglecting the separation of the impacting mass from the rod, boundary condition (a) was already considered in a previous work of Schwarz et al. (2010a). Taking the separation condition into account, boundary condition (a) results in a physically and mathematically very interesting problem, which will be solved below.
The paper is organized as follows: In Sec. 2, the geometrical setting of the model and the two different boundary conditions are introduced, and the mathematical problems to be solved are framed. The proceeding for the analytical solution of the problems on the basis of the Laplace transformation is detailed in Sec. 3. Examples of stress and displacement development for typical parameters are given in Sec. 4. The results are discussed in Sec. 5. Conclusions are presented in Sec. 6. The appendices complement the work by a review of relevant properties of the Laplace transformation, a consistent solution technique for a part of the problem which was treated in detail but with a different technique in Schwarz et al. (2010a), and some technical details.

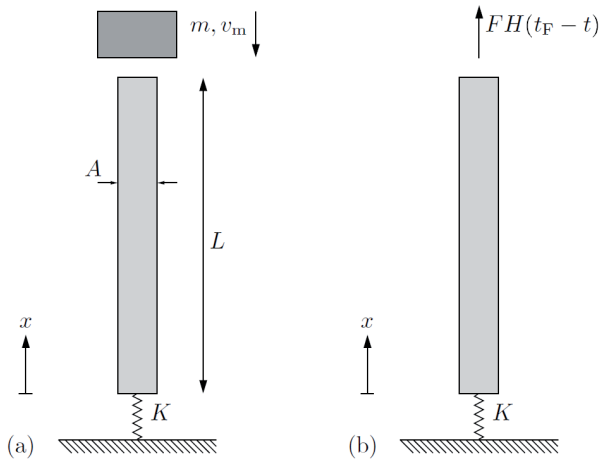

Figure 1: Sketch of the geometrical setting and applied boundary conditions (a) and (b) of the considered stamping model.

2 Problem Formulation

2.1 Geometrical Setting and Model Assumptions

For the stamping process, the model setup as sketched in Fig. 1 with two different boundary conditions (a) and (b) is considered. As stamping tool, a rod of length L, spatially constant cross-section A and a mass density ρ is considered. The elastic modulus of the rod material is E, hence its one-dimensional wave propagation speed is $c_0 = \sqrt{E/\rho}$. For the sake of simplicity the mechanical model of the rod is one-dimensional (longitudinal coordinate x). Taking into account transversal wave propagation in the rod significantly complicates the problem as was shown by the numerical study performed by Danzer et al. (2000), the references in Werner and Fischer (1995) or the publications by Skalak (1957), Valeš et al. (1996), Alterman and Karal (1970) and Boström (2000).
The rod is mounted at its lower (bottom) end $(x = 0)$ to the ground by a spring of stiffness K. At time $t = 0$ the rod is (a) either hit at its upper end by a rigid body of mass m moving downwards at a velocity v_m (absolute value) or is (b) excited by application of a force F enduring for a finite time t_F, Fig. 1.
Within a small strain setting, the displacement of (a cross section of) the rod in longitudinal direction is $u(x,t)$, the according strain is $\varepsilon = \partial u/\partial x$. The stamping tool is supposed to deform purely elastic, hence stress is related to strain via Hooke's law according to $\sigma = E\varepsilon$. Damping of any kind is not considered, since we are interested in the maximum stress in the rod occurring shortly after the impact (worst-case estimate). Furthermore, a backspring (separation) of the rod from its counterpart (spring) will not be treated in this work.

2.2 Some Remarks on Modelling the Workpiece as a Spring

The very purpose of stamping is the plastic deformation of the workpiece. So an apparent point of criticism on the presented model concerns the reasonability of substituting the workpiece by a spring.
As an example stamping process let us consider the production of coins. The pronounced elevation of the rim of the coin is not a result of the stamping, but of a preceding forming step. The plastic deformation due to the stamping of the coin's emblem is therefore only of the order of a few %, and most of the workpiece's (=coin's) volume reacts elastically to the stamping. For a qualitative estimation we put the deformation produced by stamping on a level with that in indentation experiments. A typical estimation for the correlation of the size l of the plastic zone and the radius r of a spherical indenter in an indentation experiment (the latter corresponding to the visible recess in stamping) is $l \sim 3r$, see Sundararajan and Tirupataiah (2006). If we devolve this in by a simple estimate to the stamping application, an imprint on 70 % of the surface by 5 % of the workpiece's thickness would still affect plastically only $\sim$10 % of its volume.
For another typical stamping process, the branding of wrought material, the fraction of stamping depth to material thickness is even much smaller. The plastic zone affects then only a truly negligible portion of the workpiece.
Finally, plastic dissipation would only moderate the critical loading effects on the tool considered in this paper. Hence, modelling the contact to the workpiece by mounting the rod to a spring is considered admissible for the considered worst-case estimate.

2.3 Governing Equations

The equation of motion, neglecting the small weight of the rod[1], is

$$c_0^2 \frac{\partial^2 u}{\partial x^2} = \frac{\partial^2 u}{\partial t^2}\,,\ u = u(x,t)\,. \tag{1}$$

The initial conditions are

$$u(x,0) = 0\,, \quad \frac{\partial u}{\partial t}\Big|_{t=0} = \dot{u}(x,0) = 0. \tag{2}$$

At $x = 0$ the force on the elastic support (the spring), $Ku(0,t)$, must be equal to that in the rod, $A\sigma(0,t) = EA\varepsilon(0,t)$. Introducing $\kappa = EA/K$, the boundary condition at $x = 0$ is

$$u(0,t) = \kappa \frac{\partial u}{\partial x}\Big|_{x=0} = \kappa u'(0,t)\,. \tag{3}$$

We consider two different impact scenarios, resulting in two different boundary conditions (a) and (b) at $x = L$.

(a) In case that the stamping is initiated by the impact of a falling mass m, the equation of motion of the falling mass must be regarded at $x = L$

$$m\ddot{u}(L,t) = -A\sigma(L,t) - mg \tag{4}$$

together with the initial conditions at $x = L$

$$u(L,0) = 0\,, \quad \dot{u}(L,0) = -v_{\mathrm{m}} \tag{5}$$

where v_{m} is the absolute value of the mass velocity, assumed to be oriented in negative x-direction. The quantity $\sigma(L,t) = Eu'(L,t)$ is the longitudinal stress at the top end of the rod ($x = L$), acting as tensile stress in the positive direction.
Contact exists, however, only for that time period, when $\sigma(L,t)$ is a compressive stress ($\sigma < 0$). A separation of the mass from the rod will take place at that time instant t_{c} for which

$$\sigma(L,t_{\mathrm{c}}) = 0 \quad \text{and} \quad \dot{\sigma}(L,t_{\mathrm{c}}) > 0\,. \tag{6}$$

This condition can be denominated as ‘separation condition’.
Taking this lift-off of the impacting mass into account, the boundary condition (4) has to be phrased as

$$-\frac{EA}{m}u'(L,t) = (g + \ddot{u}(L,t)) \cdot (H(t) - H(t-t_{\mathrm{c}}))\ ,\ \text{where} \tag{7}$$

$$H(\xi) = \begin{cases} 0\,, & \xi < 0\,, \\ 1\,, & \xi \geq 0\,, \end{cases} \text{ is the Heaviside Unit-Step function}\,.$$

(b) In case that the stamping is initiated by application of a force at $x = L$, initial and boundary conditions at the upper end of the rod change. For the considered excitation with $F(t) = F < 0$ being constant for $0 < t \leq t_{\mathrm{F}}$, and equal to zero for $t > t_{\mathrm{F}}$, the boundary condition can be specified as

$$EAu'(L,t) = F \cdot (H(t) - H(t-t_{\mathrm{F}}))\ . \tag{8}$$

3 Analytical Solution

The displacement function $u(x,t)$ that complies with the partial differential equation system (1 - 3) together with boundary conditions (5, 7) or (8) will be determined as follows. First, the problem is transformed into the Laplace image space, where it reduces to an ordinary differential equation in x which can be easily solved. Secondly, the solution $u(x,t)$ is restored from the image space solution $\mathcal{U}(x,s)$ by the inverse Laplace transformation. While

[1] in the sense that the weight of the rod is small compared to other forces in the system

the first step requires more or less only standard methods, rather sophisticated techniques have to be applied for the second one.

3.1 Solution in the Laplace Transformation Space

For the solution of the problem the standard Laplace transformation is used. Appendix A summarizes some of its properties that are considered relevant for the understanding of the subsequent calculations.
The partial differential equation (1) with the initial conditions (2) can be transformed from the time domain (t) together with the boundary conditions (3) and (a) (5, 7) or (b) (8) into the Laplace image space (s). With $\mathcal{U}(x,s) = \mathcal{L}[u(x,t)]$, one can rewrite the governing equations for the model with boundary conditions (a) or (b), compare Sec. 2.3, as the following ordinary differential equation in x

$$c_0^2 \mathcal{U}'' = s^2 \mathcal{U}\,, \tag{9}$$

$$\mathcal{U}(0,s) = \kappa \mathcal{U}'(0,s)\,, \tag{10}$$

$$^{(\mathrm{a})}\mathcal{U}'(L,s) = \begin{cases} -\dfrac{\alpha L}{c_0^2}\left(s^2\mathcal{U}(L,s) + \dfrac{g}{s} + v_\mathrm{m}\right) & \text{before separation}\,, \\ -\dfrac{\alpha L}{c_0^2}\left(g\cdot\dfrac{1-\mathrm{e}^{-st_\mathrm{c}}}{s} + \displaystyle\int_0^{t_\mathrm{c}} \ddot{u}(L,t)\,\mathrm{e}^{-st}\,\mathrm{d}t\right) & \text{after separation}\,. \end{cases} \tag{11a}$$

$$^{(\mathrm{b})}\mathcal{U}'(L,s) = \frac{F}{EA}\cdot\frac{1-\mathrm{e}^{-st_\mathrm{F}}}{s}\,. \tag{11b}$$

For compact notation of Eq. (11a), we defined the mass ratio $\alpha = m/\rho AL$, with ρAL being the total mass of the rod. With $\sqrt{E/\rho} = c_0$ one finds then the relation $m/EA = \alpha L/c_0^2$.
Before the separation of the impacting mass, the factor involving the Heaviside functions in Eq. (7) is equal to one, and the boundary condition can be transformed in a straight forward way to the Laplace space, see Eq. (11a) before separation. To derive the Laplace transformed boundary condition after separation, taking correctly into account the history of the impact characterized by the Heaviside functions, the original definition of the Laplace transformation was consulted

$$\begin{aligned} -\frac{c_0^2}{\alpha L}\,{}^{(\mathrm{a})}\mathcal{U}'(L,s) &= \int_0^\infty \mathrm{e}^{-st}\,(g+\ddot{u}(L,t))\cdot(H(t)-H(t-t_\mathrm{c}))\,\mathrm{d}t = \\ &= \int_0^{t_\mathrm{c}} \mathrm{e}^{-st}\,(g+\ddot{u}(L,t))\,\mathrm{d}t = \left(g\cdot\frac{1-\mathrm{e}^{-st_\mathrm{c}}}{s} + \int_0^{t_\mathrm{c}} \mathrm{e}^{-st}\,\ddot{u}(L,t)\,\mathrm{d}t\right)\,. \end{aligned} \tag{12}$$

The integrand, $\ddot{u}(L,t)$, stems from the time domain solution of the problem before the separation of the mass.
Subsequently, the abbreviations b. s. = before separation ($t \le t_\mathrm{c}$) and a. s. = after separation ($t > t_\mathrm{c}$) will be used on occasion.

The general solution of (9) can be written as

$$\mathcal{U}(x,s) = C_1 \mathrm{e}^{sx/c_0} + C_2 \mathrm{e}^{-sx/c_0}\,. \tag{13}$$

The solution in the Laplace image space, $\mathcal{U}(\delta,s)$ is given in terms of a reference time $t_0 = L/c_0$ and the dimensionless quantities $\delta = x/L \in [0;1]$ and $\tilde{\kappa} = \kappa/L$. It can be found conveniently by means of computer algebra software, e.g. MATHEMATICA, Wolfram Research (2008), by calculating the constants $C_{1,2}$ in (13) to fulfill the

boundary conditions Eqs. (10) and (11a or 11b) of the problem, resulting in[2]:

$$
{}^{(\mathrm{a})}\mathcal{U}(\delta,s) = \begin{cases} \dfrac{\alpha t_0 (g + v_\mathrm{m} s)}{s^2}\, \mathcal{G}(s) \cdot \left((1 - \tilde{\kappa} s t_0) \mathrm{e}^{(1-\delta) s t_0} - (1 + \tilde{\kappa} s t_0) \mathrm{e}^{(1+\delta) s t_0} \right) & \text{before separation,} \\ \dfrac{\alpha t_0}{s}\, \mathcal{F}(s) \cdot \Bigg[\mathrm{e}^{s t_0 (1-\delta)} (1 - \mathrm{e}^{-s t_\mathrm{c}}) \left[1 - s\tilde{\kappa} t_0 - (1 + s\tilde{\kappa} t_0) \mathrm{e}^{2 s \delta t_0} \right] \cdot & \\ \qquad \cdot \left(\dfrac{g}{s} + \dfrac{\int_0^{t_\mathrm{c}} \ddot{u}(1,t)\, \mathrm{e}^{-st}\, \mathrm{d}t}{1 - \mathrm{e}^{-s t_\mathrm{c}}} \right) \Bigg] & \text{after separation,} \end{cases} \tag{14a}
$$

$$
{}^{(\mathrm{b})}\mathcal{U}(\delta,s) = \frac{F c_0}{EA s^2}\, \mathcal{F}(s) \cdot \left[\mathrm{e}^{s t_0 (1-\delta)} (1 - \mathrm{e}^{-s t_\mathrm{F}}) \left((1 + s\tilde{\kappa} t_0) \mathrm{e}^{2 s \delta t_0} - (1 - s\tilde{\kappa} t_0) \right) \right] \tag{14b}
$$

with the functions $\mathcal{F}$ and $\mathcal{G}$ turning out to be key elements of the solution, as they represent the critical parts of the denominators in the Eqs. (14)

$$
\begin{aligned} \mathcal{G}(s) &= \left[(1 - \alpha\, s\, t_0)\, (1 - \tilde{\kappa}\, s\, t_0) + \mathrm{e}^{2\, s\, t_0}\ (1 + \alpha\, s\, t_0)\, (1 + \tilde{\kappa}\, s\, t_0) \right]^{-1}, \\ \mathcal{F}(s) &= \left[(1 - \tilde{\kappa}\, s\, t_0) + \mathrm{e}^{2\, s\, t_0}\ (1 + \tilde{\kappa}\, s\, t_0) \right]^{-1}. \end{aligned} \tag{15}
$$

Remark 1 *Equivalence of boundary conditions* (a) *and* (b)
Approximating for short impact times in the solution to boundary condition (a) *after separation, Eq. (14a), the factor that involves the integral term by a constant acceleration γ, that is*

$$
\left(g + \frac{s}{1 - \mathrm{e}^{-s t_\mathrm{c}}} \int_0^{t_\mathrm{c}} \ddot{u}(1,t)\, \mathrm{e}^{-st}\, \mathrm{d}t \right) \to \gamma\,,
$$

allows for a direct confrontation of both image space solutions for boundary conditions (a) *and* (b)*. Comparing the prefactors*

$$
-\frac{F c_0}{EA s^2} \hat{=} \frac{\alpha t_0 \gamma}{s^2} = \frac{m \gamma\, c_0}{EA s^2}
$$

and the 'core' of the solutions, it turns out, that under the given presumption, $t_\mathrm{c} = t_\mathrm{F}$, and for $F = -m\gamma$ both solutions are identical for times $t > t_\mathrm{c}$.

3.2 Solution in the Time Domain

The properties of the Laplace transform allow for a successive inverse transformation of the solution.
The inverse Laplace transformation of ${}^{(\mathrm{a})}\mathcal{U}_{\mathrm{b.s.}}$, that is for times before the separation of the impacting mass from the rod, was discussed in detail in Schwarz et al. (2010a). Note, however, that there a slightly different technique was applied for the inversion: while in Schwarz et al. (2010a) the so-called Laguerre polynomial technique was applied, involving a solution representation in terms of the Laguerre functions, here a more direct approach is presented, allowing for an elementary solution representation. For completeness, application of the present technique to the part before separation, which was only outlined in App. C of Schwarz et al. (2010a), is specified in App. B of the present contribution. A significant advantage of this approach over the former one is the more economic evaluability of the resulting time domain solution by means of computer algebra software, especially for moderate times. For the discussion of a third, essentially different technique for the inverse transformation, which is based on the Theorem of Residues, the reader is referred to App. C of Schwarz et al. (2010a).
For the inverse Laplace transformation of ${}^{(\mathrm{a})}\mathcal{U}_{\mathrm{a.s.}}$ and ${}^{(\mathrm{b})}\mathcal{U}$ we proceed as follows: in a first step the inversion of $\mathcal{F}(s)$ is considered. Then, application of the theorems on the Laplace transformation, collected in App. A, enable the complete inversion.

[2]We then define the solution u in the time domain in terms of the dimensionsless quanitities, thus changing notation from $\ddot{u}(x,t)$ to $\ddot{u}(\delta,t)$and from $\ddot{u}(L,t)$ to $\ddot{u}(1,t)$.

3.2.1 Inverse Laplace Transformation of $\mathcal{F}(s)$

For convenient notation, we introduce a new time scale in the image space by denoting $\tilde{s} = st_0$. Then the key element $\mathcal{F}(\tilde{s})$ of the image space solution, Eq. (15) is

$$\mathcal{F}(\tilde{s}) = \frac{1}{(1-\tilde{\kappa}\,\tilde{s}) + \mathrm{e}^{2\,\tilde{s}}\,(1+\tilde{\kappa}\,\tilde{s})} = \frac{\mathrm{e}^{-2\,\tilde{s}}}{1+\tilde{\kappa}\tilde{s}}\left(1+\mathrm{e}^{-2\,\tilde{s}}\frac{1-\tilde{\kappa}\tilde{s}}{1+\tilde{\kappa}\tilde{s}}\right)^{-1} = \frac{\mathrm{e}^{-2\,\tilde{s}}\mathcal{Z}(\tilde{s})}{1+\mathrm{e}^{-2\,\tilde{s}}\mathcal{X}(\tilde{s})}\,, \tag{16}$$

where the following functions were introduced

$$\mathcal{Z}(\tilde{s}) = \frac{1}{1+\tilde{\kappa}\tilde{s}} \quad \text{and} \quad \mathcal{X}(\tilde{s}) = \frac{1-\tilde{\kappa}\tilde{s}}{1+\tilde{\kappa}\tilde{s}}\,. \tag{17}$$

It can be shown, see App. B in Schwarz et al. (2010a), that $\left|\mathrm{e}^{-2\,\tilde{s}}\mathcal{X}(\tilde{s})\right| < 1$. Hence, the term in paranthesis can be considered as limit of a geometric series, which yields the following equivalent representaion of $\mathcal{F}(\tilde{s})$

$$\mathcal{F}(\tilde{s}) = \sum_{n=0}^{\infty}(-1)^n\mathrm{e}^{-2(n+1)\,\tilde{s}}\mathcal{Z}(\tilde{s})\left[\mathcal{X}(\tilde{s})\right]^n\,. \tag{18}$$

The compliance with the Cauchy-condition, which justifies the subsequently applied commutation of the inverse Laplace operator with the (infinite but uniformly convergent) series, has been demonstrated in App. C of Schwarz et al. (2010a).
We introduce the following notation: the original functions of $\mathcal{Z}$ and $\mathcal{X}$ with respect to the Laplace transformation are $z(\tilde{t})$ and $x(\tilde{t})$, where $\tilde{t} = t/t_0$. For any non-negative integer n let x_n denote the n-fold convolution of x with itself, that is

$$x_n = x^{*n} := \underbrace{x * x * x \cdots * x}_{n\text{ times}}. \tag{19}$$

By definition $x_0 = x^{*0} = \delta$, where the singular δ-distribution $\delta(\tilde{t})$ is acting as the unit element with respect to convolution $*$. According to the convolution theorem for the Laplace transformation (Eq. (A.2)), $\mathcal{L}^{-1}[\mathcal{Z}\mathcal{X}^n] = z * x_n$. We find with the definitions in Eq. (17)

$$\begin{aligned} z(\tilde{t}) &= \frac{1}{\tilde{\kappa}}\mathrm{e}^{-\tilde{t}/\tilde{\kappa}} = z * x_0\,, \\ x(\tilde{t}) &= x_1(\tilde{t}) = \frac{2}{\tilde{\kappa}}\mathrm{e}^{-\tilde{t}/\tilde{\kappa}} - \delta(\tilde{t}) \;\curvearrowright\; z * x_1 = \frac{1}{2\tilde{\kappa}}\mathrm{e}^{-\tilde{t}/\tilde{\kappa}}\left(\frac{4\tilde{t}}{\tilde{\kappa}} - 1\right). \end{aligned} \tag{20}$$

Utilising Eq. (A.3) and the correspondency $[\mathrm{e}^{-ct}]^{*m} = \frac{t^{m-1}}{(m-1)!}\,\mathrm{e}^{-ct}\,,\ c,t>0,\ m\in\mathbb{N}$, yields

$$\begin{aligned} x_n(\tilde{t}) &= \left[\frac{2}{\tilde{\kappa}}\mathrm{e}^{-\tilde{t}/\tilde{\kappa}} - \delta(\tilde{t})\right]^{*n} = \sum_{k=0}^{n}(-1)^{n-k}\binom{n}{k}\left[\frac{2}{\tilde{\kappa}}\mathrm{e}^{-\tilde{t}/\tilde{\kappa}}\right]^{*k} * \left[\delta(\tilde{t})\right]^{*(n-k)} = \\ &= (-1)^n\delta(\tilde{t}) + \sum_{k=1}^{n}(-1)^{n-k}\binom{n}{k}\left(\frac{2}{\tilde{\kappa}}\right)^k\left[\mathrm{e}^{-\tilde{t}/\tilde{\kappa}}\right]^{*k} = (-1)^n\delta(\tilde{t}) + \sum_{k=1}^{n}\binom{n}{k}\left(\frac{2}{\tilde{\kappa}}\right)^k\frac{(-1)^{n-k}}{(k-1)!}\,\tilde{t}^{k-1}\mathrm{e}^{-\tilde{t}/\tilde{\kappa}}\,, \end{aligned} \tag{21}$$

and in consequence

$$\begin{aligned} \mathcal{L}^{-1}[\mathcal{Z}\mathcal{X}^n] =: f_n(\tilde{t}) = z(\tilde{t}) * x_n(\tilde{t}) &= \frac{(-1)^n}{\tilde{\kappa}}\mathrm{e}^{-\tilde{t}/\tilde{\kappa}} + \sum_{k=1}^{n}\frac{(-1)^{n-k}}{\tilde{\kappa}\,k!}\binom{n}{k}\left(\frac{2}{\tilde{\kappa}}\right)^k\tilde{t}^k\mathrm{e}^{-\tilde{t}/\tilde{\kappa}} = \\ &= \sum_{k=0}^{n}\lambda_{nk}\tilde{t}^k\mathrm{e}^{-\tilde{t}/\tilde{\kappa}}\,, \text{ where } \lambda_{nk} = \frac{(-1)^{n-k}}{\tilde{\kappa}\,k!}\binom{n}{k}\left(\frac{2}{\tilde{\kappa}}\right)^k. \end{aligned} \tag{22}$$

Taking care of the remaining exponential term in Eq. (18) with the First Shift Theorem of the Laplace transforma-

tion, see Doetsch (1974), one gets

$$\mathcal{L}^{-1}[\mathcal{F}(\tilde{s})] =: f(\tilde{t}) = \sum_{n=0}^{\infty}(-1)^n f_n(\tilde{t} - 2(n+1))\,. \tag{23}$$

We presume the convention that any function $f(\xi)$ which stems from an inverse Laplace transformation is defined only for $\xi \geq 0$ and is, per definition, zero for $\xi < 0$. This implies that series elements $n \geq N$ contribute to the solution only for times $\tilde{t} \geq 2(N+1)$, such that for finite times the series in Eq. (23) is actually finite.
The according procedure for the inverse transformation of the corresponding element of ${}^{(a)}\mathcal{U}_{\mathrm{b.s.}}$ is presented in App. B.

3.2.2 Complete Inverse Laplace Transformation of the Displacement Solutions

As it proved to be convenient, and in order to be consistent, we rewrite the image space solutions for the different boundary conditions, Eqs. (14), as functions of the scaled image space variable $\tilde{s} = st_0$, introducing thereby $\tilde{t}_{\mathrm{c}} = t_{\mathrm{c}}/t_0$ and $\tilde{t}_{\mathrm{F}} = t_{\mathrm{F}}/t_0$:

$${}^{(\mathrm{a})}\mathcal{U}(\delta,\tilde{s}) = \begin{cases} \dfrac{\alpha t_0^2(gt_0 + v_{\mathrm{m}}\tilde{s})}{\tilde{s}^2}\,\mathcal{G}(\tilde{s}) \cdot \Big((1-\tilde{\kappa}\tilde{s})\mathrm{e}^{(1-\delta)\tilde{s}} - (1+\tilde{\kappa}\tilde{s})\mathrm{e}^{(1+\delta)\tilde{s}}\Big) & \text{before separation,} \\ \dfrac{\alpha t_0^3}{\tilde{s}}\mathcal{F}(\tilde{s})\Bigg[\mathrm{e}^{\tilde{s}(1-\delta)}(1-\mathrm{e}^{-\tilde{s}\tilde{t}_{\mathrm{c}}})\left[1-\tilde{s}\tilde{\kappa}-(1+\tilde{s}\tilde{\kappa})\mathrm{e}^{2\tilde{s}\delta}\right]\cdot \\ \qquad\qquad \cdot\left(\dfrac{g}{\tilde{s}} + \dfrac{\int_0^{\tilde{t}_{\mathrm{c}}}\ddot{u}(1,\tilde{t})\,\mathrm{e}^{-\tilde{s}\tilde{t}}\,\mathrm{d}\tilde{t}}{1-\mathrm{e}^{-\tilde{s}\tilde{t}_{\mathrm{c}}}}\right)\Bigg] & \text{after separation,} \end{cases} \tag{24a}$$

$${}^{(\mathrm{b})}\mathcal{U}(\delta,\tilde{s}) = \frac{Fc_0t_0^2}{EA\tilde{s}^2}\mathcal{F}(\tilde{s})\left[(1-\mathrm{e}^{-\tilde{s}\tilde{t}_{\mathrm{F}}})\left((1+\tilde{s}\tilde{\kappa})\mathrm{e}^{\tilde{s}(1+\delta)} - (1-\tilde{s}\tilde{\kappa})\mathrm{e}^{\tilde{s}(1-\delta)}\right)\right] \tag{24b}$$

To finalize the inverse Laplace transformation of ${}^{(\mathrm{b})}\mathcal{U}$, Eq. (A.4) is applied, which is in our case

$$\mathcal{L}^{-1}\Big[\frac{1}{\tilde{s}^n}\mathrm{e}^{-a\tilde{s}}\mathcal{F}(\tilde{s})\Big] = \frac{1}{t_0}\int_0^{\tilde{t}}(\tilde{t}-\tau)^{n-1}f(\tau-a)\,\mathrm{d}\tau\,. \tag{25}$$

The variable a substitutes the different factors in the exponential functions occuring.
However, inverting ${}^{(\mathrm{a})}\mathcal{U}_{\mathrm{a.s.}}$ requires an additional consideration. The formulation of the boundary condition Eq. (7), which takes into account the separation condition for the impacting mass by means of the Heaviside unit-step function, is the source of the integral term in Eq. (24a). This term is awkward: it involves the solution u in the time domain for earlier times, and it is actually existing in the Laplace transformation space only after integration. Inverse Laplace transformation can be realized by applying the transformation rule for periodic functions, yielding

$$\mathcal{L}^{-1}\left[\frac{1}{1-\mathrm{e}^{-\tilde{s}\tilde{t}_{\mathrm{c}}}}\int_0^{\tilde{t}_{\mathrm{c}}}\ddot{u}(1,\tilde{t})\,\mathrm{e}^{-\tilde{s}\tilde{t}}\,\mathrm{d}\tilde{t}\right] = \ddot{u}^{\mathrm{per}}(1,\tilde{t}) := \ddot{u}(1,\tilde{t}), \text{recurrent with period } \tilde{t}_{\mathrm{c}}\,. \tag{26}$$

Subsequent application of the convolution theorem, Eq. (A.2), yields

$$\mathcal{L}^{-1}\left[\mathcal{F}(\tilde{s})\cdot\left(\frac{1}{1-\mathrm{e}^{-\tilde{s}\tilde{t}_{\mathrm{c}}}}\int_0^{\tilde{t}_{\mathrm{c}}}\ddot{u}(1,\tilde{t})\,\mathrm{e}^{-\tilde{s}\tilde{t}}\,\mathrm{d}\tilde{t}\right)\right] = \int_0^{\tilde{t}} f(\tau)\cdot\ddot{u}^{\mathrm{per}}(1,\tilde{t}-\tau)\,\mathrm{d}\tau =: \psi(\tilde{t})\,. \tag{27}$$

By applying Eq. (A.4) one obtains a complete inverse transformation of the solution ${}^{(\mathrm{a})}\mathcal{U}_{\mathrm{a.s.}}$.

Finally, the solutions in the time domain for the two considered boundary conditions (a) and (b) are

$$
{}^{(\mathrm{a})}u(\delta,\tilde{t}) =
$$

$$
= \begin{cases}
\text{see Schwarz et al. (2010a) or App. B}\,, & \text{b. s., } \tilde{t} \le \tilde{t}_\mathrm{c} \\
-\alpha t_0^2 \Big\{ g\Big[\tilde{\kappa}\int_0^{\tilde{t}} \big(f(\tau+1+\delta)+f(\tau+1-\delta)-f(\tau+1+\delta-\tilde{t}_\mathrm{c})-f(\tau+1-\delta-\tilde{t}_\mathrm{c})\big)\mathrm{d}\tau + \\
\quad + \int_0^{\tilde{t}} (\tilde{t}-\tau)\big(f(\tau+1+\delta)-f(\tau+1-\delta)-f(\tau+1+\delta-\tilde{t}_\mathrm{c})+f(\tau+1-\delta-\tilde{t}_\mathrm{c})\big)\mathrm{d}\tau\Big] + \\
\quad + \tilde{\kappa}\big(\psi(\tau+1+\delta)+\psi(\tau+1-\delta)-\psi(\tau+1+\delta-\tilde{t}_\mathrm{c})-\psi(\tau+1-\delta-\tilde{t}_\mathrm{c})\big) + \\
\quad + \int_0^{\tilde{t}} \big(\psi(\tau+1+\delta)-\psi(\tau+1-\delta)-\psi(\tau+1+\delta-\tilde{t}_\mathrm{c})+\psi(\tau+1-\delta-\tilde{t}_\mathrm{c})\big)\mathrm{d}\tau \Big\}, & \text{a. s., } \tilde{t} > \tilde{t}_\mathrm{c}
\end{cases}
\tag{28a}
$$

$$
{}^{(\mathrm{b})}u(\delta,\tilde{t}) = \frac{Fc_0t_0}{EA}\Big[\tilde{\kappa}\int_0^{\tilde{t}} \big(f(\tau+1+\delta)+f(\tau+1-\delta)-f(\tau+1+\delta-\tilde{t}_\mathrm{F})-f(\tau+1-\delta-\tilde{t}_\mathrm{F})\big)\,\mathrm{d}\tau + \\
+ \int_0^{\tilde{t}} (\tilde{t}-\tau)\,\big(f(\tau+1+\delta)-f(\tau+1-\delta)-f(\tau+1+\delta-\tilde{t}_\mathrm{F})+f(\tau+1-\delta-\tilde{t}_\mathrm{F})\big)\,\mathrm{d}\tau\Big] \tag{28b}
$$

3.2.3 The Separation Time t_c within Boundary Condition (a)

So far, the separation time t_c in boundary condition (a) has been treated as unknown. We analyzed the solution valid before the impacting mass separates from the rod, App. B, assuming reasonable parameter values. It could be rigorously shown that the stress at the upper end of the rod turns into a tensile stress right when the stress wave, initiated solely by the impacting mass at $t = 0$, comes back to this end after having been reflected at the lower end. This takes exactly the time $\tilde{t}_\mathrm{c} = 2$. Details of this analysis are given in App. C. A further discussion is deferred to Sec. 5.

As has been pointed out subsequent to Eq. (23) and thoroughly discussed in Schwarz et al. (2010a), the solution to boundary condition (a) for times $\tilde{t} \le 2 = \tilde{t}_\mathrm{c}$ is exactly defined by considering only the first element, $n = 0$, of the series representation of the solution Eq. (B.12). In this case, its second derivative with respect to t at the position $x = L$ (i. e. $\delta = 1$) can be explicitly stated for $\tilde{t} \le 2$, and provides the periodic function $\ddot{u}^\mathrm{per}$

$$
\ddot{u}^\mathrm{per}(1,\tilde{t}) = \left(\frac{v_\mathrm{m}}{t_0\alpha} - g\right) \mathrm{e}^{-\dfrac{(\tilde{t} \bmod \tilde{t}_\mathrm{c})}{\alpha}}\,, \tag{29}
$$

where the modulo-calculus was used to define the periodic function for all $\tilde{t}$.

4 Results

The results for the stamping model depicted in the following graphs are based on a common set of geometry and material parameters:
$E = 220\,\mathrm{GPa},\ \rho = 7750\,\mathrm{kg/m^3},\ A = 10\,\mathrm{cm^2},\ L = 1\,\mathrm{m}$. The parameter $\tilde{\kappa} = EA/KL$, defining the (inverse) spring stiffness, was kept variable. Except for the graph in Fig. 3b, which serves as a demonstration that also a fully numerical solution as hyperbolic partial differential equation system is possible, see Schwarz et al. (2010a), all graphs were produced by evaluation of the above given analytical solutions using the software MATHEMATICA, Wolfram Research (2008).

4.1 Boundary Condition (a)

For the impacting mass $m = 100\,\mathrm{kg}$ and $v_\mathrm{m} = 10\,\mathrm{m/s}$ are used. The gravitational acceleration is approximated as $g = 10\,\mathrm{m/s^2}$. In both Figs. 2 and 3, that part of the solution before the separation of the impacting mass affects the respective position in the rod (marked by a dashed line style) coincides with the results presented in the preceding

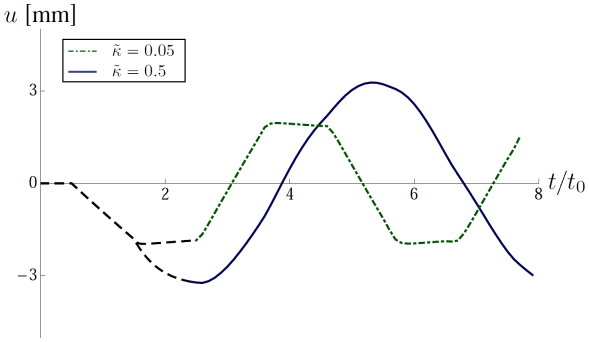

(a) In the center of the rod, $\delta = 0.5$.

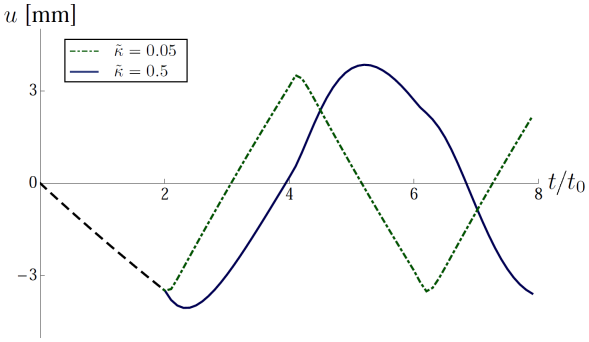

(b) At the upper end of the rod, $\delta = 1$.

Figure 2: Boundary condition (a): Displacement vs. time for different values of the spring stiffness, $\tilde{\kappa} = 0.05$ (dot-dashed) and $\tilde{\kappa} = 0.5$ (solid). The dashed segment at the beginning of the curves (i. e. (a) for $t < 2.5t_0$ and (b) for $t < 2t_0$) marks the part of the solution before the separation of the impacting mass has an influence on the respective position δ in the rod.

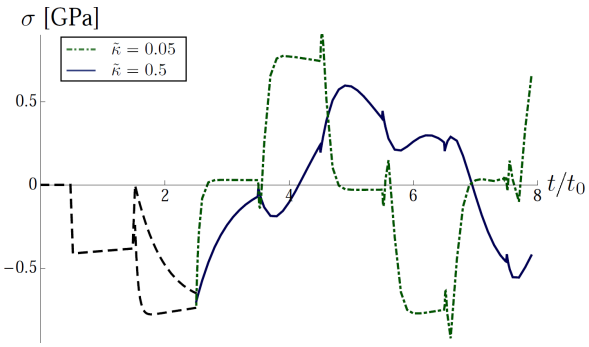

(a) Symbolic / analytical solution by MATHEMATICA.

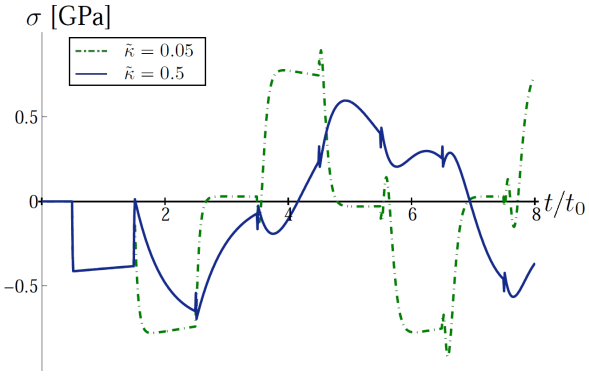

(b) Numerical solution by MATLAB The MathWorks (2010).

Figure 3: Boundary condition (a): Stress vs. time in the center of the rod ($\delta = 0.5$) for different values of the spring stiffness, $\tilde{\kappa} = 0.05$ (dot-dashed) and $\tilde{\kappa} = 0.5$ (solid). The dashed segment at the beginning of the curves in subfigure (a), i. e. for $t < 2.5t_0$, marks the part of the solution before the separation of the impacting mass has an influence on the considered position $\delta = 0.5$ in the rod. In subfigure (b), for validation a fully numerically calculated solution is shown. For details on the numerical method see Schwarz et al. (2010a).

work (Schwarz et al., 2010a, Fig. 4). After the separation of the mass[3], the results differ significantly, and resemble those found in the present work for boundary condition (b). The impacting mass then acts like an impact in the literal sense, not further influencing the rod's response by the additional weight that stores a considerable amount of energy when not lifting off. Merely the spikes in stress appearing in Fig. 3 in comparison to Fig. 4b at instants $(2.5 + j)t_0$, $j \in \mathbb{N}_0$, remind one of the differing history.

4.2 Boundary Condition (b)

In order to provide comparability with the results due to boundary condition (a), an effective period of length $t_\mathrm{F} = 2t_0$ was specified ($\hat{=}$ retention time of the mass on the rod). The force exerted at the upper end of the rod was chosen to be $F = -350,000\,\mathrm{N}$. Except for a time shift, i. e. for $t > 2t_\mathrm{F}$, and a sign-inversion, the results depicted in Figs. 4a and 4b look alike those presented in (Schwarz et al., 2010a, Fig. 2) for what was denoted the Valve-case (rod with uniform initial velocity being caught by the spring at its lower end). By application of the load $F(t)$ the rod is virtually accelerated to some 'initial velocity', too, such that from the time on when the introduced stress wave reaches the lower end of the rod the response is equivalent to that for the Valve-case.

[3] Actually the impacting mass is removed from the system after the separation, so no possible subsequent impact is taken into account in the model.

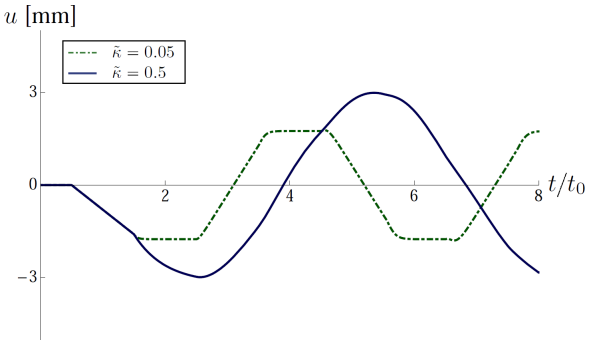

(a) Displacement vs. time.

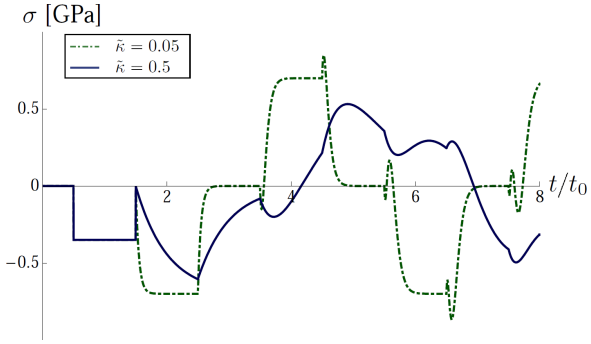

(b) Stress vs. time.

Figure 4: Boundary condition (b): Displacement and stress vs. time in the center of the rod ($\delta = 0.5$) for different values of the spring stiffness, $\tilde{\kappa} = 0.05$ (dot-dashed) and $\tilde{\kappa} = 0.5$ (solid).

Remark 2 *Eigenfrequency of the system. Assuming for a spring which is very soft compared to the stiffness of the rod the system as spring-mass-oscillator (harmonic oscillator) in the most simple sense, the period T (of the periodic displacement of the rod) would be expected to be*

$$T = \frac{2\pi}{\omega} = 2\pi\sqrt{\frac{m_{\text{rod}}}{K}} = 2\pi\sqrt{\frac{\rho AL\kappa}{EA}} = \cdots = 2\pi t_0\sqrt{\tilde{\kappa}}\,.$$

As shown in Fig. 5a, the development of the rigid body displacement[4] $u_{\text{S}}(t) = \frac{1}{L}\int_0^L u(x,t)\,\mathrm{d}x$ *is in accordance with this correlation for values of $\tilde{\kappa} > 5$. Obviously the factor 4 in $\tilde{\kappa}$ gives the factor 2 in the period T of the displacement development. For instance, for $\tilde{\kappa} = 20$ the above formula yields $T = 28.1\,t_0$, which coincides well with the observed development of the rigid body displacement and the stress in the center of the rod, Fig. 5b.*

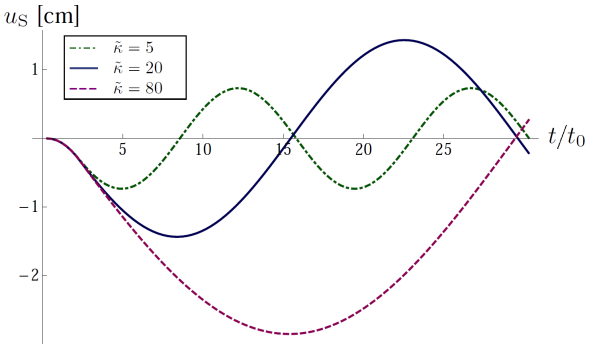

(a) Rigid body displacement vs. time.

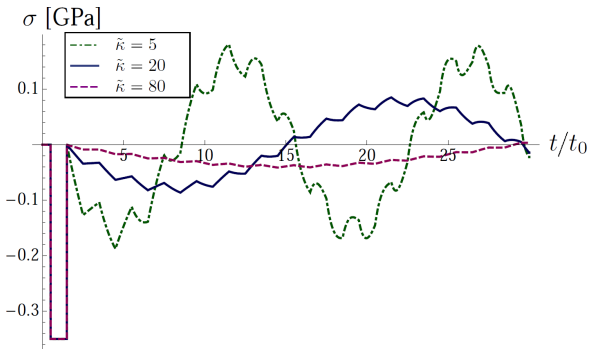

(b) Stress vs. time in the center of the rod ($\delta = 0.5$).

Figure 5: Evolution of rigid body displacement and stress (exemplarily at $\delta = 0.5$) for boundary condition (b) and different values of the spring stiffness: $\tilde{\kappa} = 5$ (dot-dashed), $\tilde{\kappa} = 20$ (solid) and $\tilde{\kappa} = 80$ (dashed).

In the limit case $K \to 0$ resp. $\tilde{\kappa} \to \infty$, the solution approaches that for a rod with free lower end. The amount of energy absorbed by the spring tends to zero, and only the force impulse oscillates in the rod, being mirrored at both free ends. The displacement development resembles a straightly descending line, thus representing the macroscopic displacement of the rod. The wave length observed in Fig. 5a would, for this limit case, tend to infinity.

5 Discussion

Exploiting the special structure of the solution in the image space, the solution in the time-domain can be given in closed form. It can be phrased as infinite series of which for finite times only a finite number of elements add to

[4]The rigid body displacement is the displacement of the center of mass of the rod, u_{S}, which is numerically calculated as mean of the displacements $u(\delta_i, t)$ at 100 equidistant positions δ_i in the rod.

the solution, see Eqs. (23) and (28).
We believe, that especially the exploration of different analytic solution strategies and representations, as specified here and in previous publications, gives valuable insight into the structure of the solution and the characteristics of the problem. The presented technique provides a closed form solution for finite times, i. e. exact results, and allows for efficient numerical evaluation. Complementarily, the approach via the Theorem of Residues, see App. C of Schwarz et al. (2010a), enables a detailed investigation of the analytic properties of the result.
It is already evident from the rather short time interval in which the solution was evaluated that the stress profile for rather stiff barriers, e. g. $\tilde{\kappa} = 0.05$, still resembles that for completely stiff barriers, but is superposed by additional stress pulses, Figs. 3 and 4b. As could be shown in Werner and Fischer (1995) for the valve problem, there is a critical value of $\tilde{\kappa}$ of approximately 0.05 for which this extra stress is maximal. In the worst case, the stress was found to reach approximately $1.26 \times \bar{\sigma}$, where $\bar{\sigma} = Ev_{\mathrm{m}}/c_0$ is the maximum stress in the rod for a stiff barrier ($\tilde{\kappa} \to 0$). In the center of the rod, for example, this extra stress arrives at times $\tilde{t} = 3.5, 4.5, 5.5, \ldots$. Its origin is, of course, the barrier, which repeatedly stores some energy and continuously re-supplies it to the rod in a small time interval. As this extra stress is then partially stored and retransmitted from the spring, too, the number of peaks in the superposed stress pulse increases with the number of cycles.
A partial verification of the final result, Eq. (28a, before separation), can be provided for the limit case $\tilde{\kappa} \to 0$, which represents an infinitely stiff spring behaving equivalently to a rigid barrier. Hu and Eberhard (2001) presented an analytic solution for an equivalent problem: the impact of a rigid mass on an elastic rod, which is fixed at the other end. It is defined according to Eqs. (1 - 3) and (4, 5), too, with the only difference that no gravity field is included, i. e. $g = 0$. On the basis of the general solution for the wave equation according to d'Alembert, they derive an analytic solution of the form 'polynomial $\times$ exponential function', compare Eq. (B.8). However, Hu and Eberhard (2001) do not give a closed form solution. The results on the duration of contact of impacting mass and rod as well as on the maximum stress in the rod (both investigated with respect to varying mass ratios α) that are presented by Hu and Eberhard (2001) are perfectly reproduced by our solution, Eq. (28), in the limit case $\tilde{\kappa} \to 0$. This finding does not contravene the earlier discussion on the separation time being qual to $\tilde{t}_{\mathrm{c}} = 2$, Sec. 3.2.3. In the limit case $\tilde{\kappa} \to 0$, the effect that the spring lets the lower end of the rod act as a free end in at first moment, see also App. C, is no longer resolvable, and the actual duration of contact can be determined.

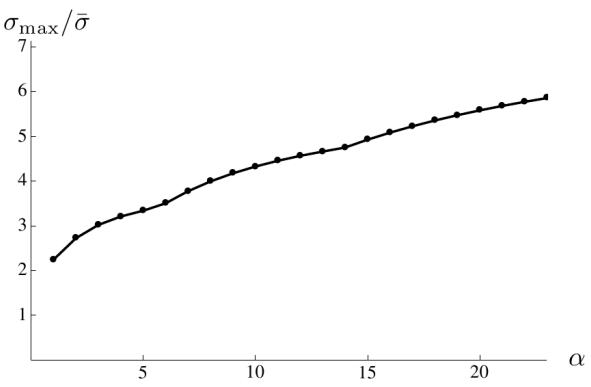

(a) Duration of contact t_{c} as a function of the mass ratio α, compare Hu and Eberhard (2001), Fig. 3.

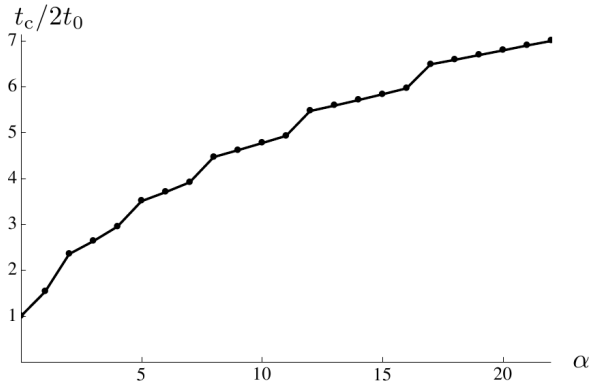

(b) Maximum dimensionless stress in the rod, found at $x = 0$, as a function of α, compare Hu and Eberhard (2001), Fig. 5.

Figure 6: Reproduction of the results of Hu and Eberhard (2001) from Eq. (28a, before separation) in the limit case $\tilde{\kappa} \to 0$ for discrete values of the mass ratio α. Note that the variable α in this contribution and α in Hu and Eberhard (2001) denote reciprocal values.

Various authors, e. g. Matuk (1979) or Shi (1998a,b), have been treating impact problems on the basis of elastic rods, too. However, no tangible, general results have been specified in these contributions. Partly, recursion rules are indicated, partly only very special aspects of the impact problem, e. g. the coefficient of restitution, were studied.

6 Conclusions

The application of the analytical solution technique presented in this work to a simple model for a stamping process provides exact and therefore incontestable results for the stress development in the tool. The compliant workpiece thereby has been modelled by a spring.
The solution technique is based on the Laplace transformation of the wave equation for the displacement of cross-

sections of the rod. Calculation of the respective solution in the Laplace image space is straight-forward, however the inverse transformation demands some skills, especially when considering the separation of the impacting mass from the rod. The results for the limit case of an infinitely stiff spring are perfectly in agreement with those found in the literature for a rigid barrier. However, the spring was introduced actually as a model for a non-rigid bedding. Its action may, under certain circumstances, be put on a level with that of a short, second bar, whose action might be easier to understand, and which is actually a more realistic model to the real workpiece, e.g. a coin. This correspondence is currently being investigated.

A Important Properties of the Laplace Transform

In the present contribution we use the Laplace transformation as a convenient tool for the solution of a partial differential equation with nontrivial boundary conditions. Rather than going further into the mathematical details, for which the reader is referred to the literature, e.g. Doetsch (1974), we would like to summarize only few important properties of the Laplace transformation that are relevant for the presented calculations. We use the following notation:
The Laplace transformation, denoted by the operator $\mathcal{L}$, maps the function $f = f(t) : \mathbb{R} \to \mathbb{R}$ to its Laplace transformed counterpart $\mathcal{F} = \mathcal{F}(s) : \mathbb{C} \to \mathbb{C}$

$$\mathcal{L}\left[f(t)\right] = \mathcal{L}\left[f\right](s) = \mathcal{F}(s) := \int_0^\infty \mathrm{e}^{-st} f(t)\,\mathrm{d}t\,. \tag{A.1}$$

For a brief representation of the solution in the time domain, we utilise that any function $f(\xi)$ which stems from an inverse Laplace transformation is defined only for $\xi \geq 0$ and, per definition, zero for $\xi < 0$.

Convolution Theorem

For the inverse Laplace transformation of the product of two functions $\mathcal{F}(s)$ and $\mathcal{G}(s)$ with the respective original functions $f(t)$ and $g(t)$ the convolution theorem holds

$$\mathcal{L}^{-1}\left[\mathcal{F}(s)\cdot\mathcal{G}(s)\right] = f(t) * g(t) = \int_0^t f(t-\tau)\cdot g(\tau)\,\mathrm{d}\tau = \int_0^t g(t-\tau)\cdot f(\tau)\,\mathrm{d}\tau\,. \tag{A.2}$$

Since convolution is a commutative and associative binary operation, which in addition is distributive with respect to the operation $+$, a binomial theorem holds

$$(f+g)^{*n} = \sum_{k=0}^{n} \binom{n}{k} f^{*k} * g^{*(n-k)}\,. \tag{A.3}$$

Combination of the Rules

In the present case we have to apply several of the common transformation rules, that were summarized in Schwarz et al. (2010a), simultaneously. As the order of application is of major importance, we demonstrate the correct way of combination in the following form

$$\mathcal{L}^{-1}\left[\frac{1}{s^n}\cdot\mathrm{e}^{-cs}\cdot\frac{1}{a}\mathcal{F}\left(\frac{s}{a}\right)\cdot\frac{1}{b}\mathcal{G}\left(\frac{s}{b}\right)\right] = t^{n-1} * q(t-c) = \int_c^t (t-\tau)^{n-1}\cdot q(\tau-c)\,\mathrm{d}\tau\,, \tag{A.4}$$

where $q(\xi) = \int_0^\xi f(a(\xi-\eta))\cdot g(b\eta)\,\mathrm{d}\eta\,.$

B The Solution before the Separation of the Impacting Mass

Different from the approach presented in Sec. 3.2 for the inverse Laplace transformation of $\mathcal{F}$ exploiting the convolution theorem, in Schwarz et al. (2010a) the inverse Laplace transformation of the key element $\mathcal{G}$ of ${}^{(\mathrm{a})}\mathcal{U}_{\mathrm{b.s.}}$, Eq. (15), was derived in terms of Laguerre functions. In this section, the above presented, in many aspects

superior, technique is applied to ${}^{(\mathrm{a})}\mathcal{U}_{\mathrm{b.s.}}$, too. We provide explicitly in the framework of this paper the solution of the problem in the time domain before the separation of the impacting mass, Eq. (28a).

Recall the solution to problem (a) before separation in terms of $\tilde{s} = st_0$, Eq. (24a), however slightly rearranged

$$ {}^{(\mathrm{a})}\mathcal{U}(\delta,\tilde{s})_{\mathrm{b.s.}} = \frac{\alpha t_0^2(gt_0 + v_{\mathrm{m}}\tilde{s})}{\tilde{s}^2}\,\mathcal{H}(\tilde{s})\cdot\left[(1-\tilde{\kappa}\tilde{s})\mathrm{e}^{-\delta\tilde{s}} - (1+\tilde{\kappa}\tilde{s})\mathrm{e}^{\delta\tilde{s}}\right]\,, \tag{B.1} $$

where we introduce the key element of this solution representation $\mathcal{H}(\tilde{s})$ as

$$ \mathcal{H}(\tilde{s}) = \mathrm{e}^{-\tilde{s}}\mathcal{Z}(\tilde{s})\left[1+\mathrm{e}^{-2\tilde{s}}\mathcal{X}(\tilde{s})\right]^{-1}\,, \tag{B.2} $$

with

$$ \mathcal{Z}(\tilde{s}) = \frac{1}{(1+\alpha\tilde{s})(1+\tilde{\kappa}\tilde{s})}\,,\quad \mathcal{X}(\tilde{s}) = \frac{(1-\alpha\tilde{s})(1-\tilde{\kappa}\tilde{s})}{(1+\alpha\tilde{s})(1+\tilde{\kappa}\tilde{s})}\,. \tag{B.3} $$

We denote the original functions of $\mathcal{H}(\tilde{s}), \mathcal{X}(\tilde{s})$ and $\mathcal{Z}(\tilde{s})$ with respect to the Laplace transformation as $h(\tilde{t}), x(\tilde{t})$ and $z(\tilde{t})$, where again $\tilde{t} = t/t_0$. Moreover, for shorter notation, the abbreviations $a = 1/\alpha$, $b = 1/\tilde{\kappa}$ as well as $\Gamma = 2(a+b)/(b-a)$ are introduced.
Like in Sec. 3.2, the term in brackets in the expression for $\mathcal{H}$ is interpreted as limit of a geometrical series, yielding

$$ \mathcal{H}(\tilde{s}) = \sum_{n=0}^{\infty}(-1)^n\mathrm{e}^{-(2n+1)\tilde{s}}\mathcal{Z}(\tilde{s})\mathcal{X}^n(\tilde{s})\,, \tag{B.4} $$

which can be formally inverted with respect to the Laplace transformation by application of the convolution theorem, Eq. (A.2), resulting in

$$ h(\tilde{t}) = \sum_{n=0}^{\infty}(-1)^n[z * x_n](\tilde{t}-2n-1) =: \sum_{n=0}^{\infty}(-1)^n h_n(\tilde{t}-2n-1)\,. \tag{B.5} $$

As before, $x_n := x^{*n}$ denotes the n-fold convolution of x with itself, and the Heaviside factor can be omitted respecting the remark given subsequent to Eq. (A.1). The compliance with the Cauchy-condition, which justifies the subsequently applied commutation of the inverse Laplace operator with the (infinite but uniformly convergent) series, has been demonstrated in App. C of Schwarz et al. (2010a).
For the Laplace inverse functions to $\mathcal{Z}$ and $\mathcal{X}$, Eq. (B.3), we find

$$ z(\tilde{t}) = \frac{ab}{a-b}\left(\mathrm{e}^{-b\tilde{t}} - \mathrm{e}^{-a\tilde{t}}\right)\,,\; x(\tilde{t}) = \Gamma\cdot\left(a\mathrm{e}^{-a\tilde{t}} - b\mathrm{e}^{-b\tilde{t}}\right) + \delta(\tilde{t}) =: \Gamma\cdot\zeta(\tilde{t}) + \delta(\tilde{t})\,, \tag{B.6} $$

where $\delta(\tilde{t})$ is the Dirac delta function. For calculation of the functions h_n, again the binomial theorem for the convolution, Eq. (A.3), is applied

$$ h_n(\tilde{t}) = z(\tilde{t}) * \left(\Gamma\cdot\zeta(\tilde{t}) + \delta(\tilde{t})\right)^{*n} = z(\tilde{t}) * \left(\sum_{k=0}^{n}\binom{n}{k}\left(\Gamma\cdot\zeta(\tilde{t})\right)^{*k} * \delta^{*(n-k)}\right) = $$
$$ = \sum_{k=0}^{n}\Gamma^k\cdot\binom{n}{k}\left(z(\tilde{t}) * \left[\zeta(\tilde{t})\right]^{*k}\right)\,. \tag{B.7} $$

Lengthy, but standard technical calculations provide explicit expressions for h_n in the form

$$ h_n(\tilde{t}) = \mathrm{e}^{-a\tilde{t}}p_n(\tilde{t}) - \mathrm{e}^{-b\tilde{t}}q_n(\tilde{t})\,, \tag{B.8} $$

where p_n, q_n are polynomials of order n, that can be calculated as follows

$$ p_n(\tilde{t}) = \sum_{k=0}^{n}\binom{n}{k}\Gamma^k\tilde{p}_k(\tilde{t}) \qquad \text{with} \qquad \tilde{p}_k(\tilde{t}) = \sum_{i=0}^{k}\frac{\tilde{x}_i^{(k)}}{i!}\tilde{t}^i\,, $$
$$ q_n(\tilde{t}) = \sum_{k=0}^{n}\binom{n}{k}\Gamma^k\tilde{q}_k(\tilde{t}) \qquad \text{with} \qquad \tilde{q}_k(\tilde{t}) = \sum_{i=0}^{k}\frac{\tilde{y}_i^{(k)}}{i!}\tilde{t}^i\,. \tag{B.9} $$

The coefficients $\tilde{x}, \tilde{y}$ can be calculated iteratively according to ($c := a - b$)

$$\begin{aligned}
\tilde{x}_0^{(k)} &= -\frac{ab}{c}\sum_{i=0}^{k-1}\frac{\hat{x}_i^{(k)} + (-1)^i\hat{y}_i^{(k)}}{c^{i+1}}\,, & \tilde{y}_0^{(k)} &= -\frac{ab}{c}\sum_{i=0}^{k-1}\frac{\hat{x}_i^{(k)} + (-1)^i\hat{y}_i^{(k)}}{c^{i+1}}\,,\\
\tilde{x}_l^{(k)} &= -\frac{ab}{c}\left(\hat{x}_{l-1}^{(k)} + \sum_{i=l}^{k-1}\frac{\hat{x}_i^{(k)}}{c^{i-l+1}}\right), & \tilde{y}_l^{(k)} &= \frac{ab}{c}\left(\hat{y}_{l-1}^{(k)} - \sum_{i=l}^{k-1}\frac{\hat{y}_i^{(k)} + (-1)^{i-l}}{c^{i-l+1}}\right),\\
& 1 \le l \le k-1 & & \\
\tilde{x}_k^{(k)} &= -\frac{ab}{c}\hat{x}_{k-1}^{(k)}\,, & \tilde{y}_k^{(k)} &= \frac{ab}{c}\hat{y}_{k-1}^{(k)}\,,
\end{aligned} \tag{B.10}$$

where the $\hat{x}, \hat{y}$ result with the initial values $\hat{x}_0^{(1)} = a$, $\hat{y}_0^{(1)} = b$ from

$$\begin{aligned}
\hat{x}_0^{(k+1)} &= \sum_{i=0}^{k-1}\frac{b\hat{x}_i^{(k)} + (-1)^i a\hat{y}_i^{(k)}}{c^{i+1}}\,, & \hat{y}_0^{(k+1)} &= \sum_{i=0}^{k-1}\frac{b\hat{x}_i^{(k)} + (-1)^i a\hat{y}_i^{(k)}}{c^{i+1}}\,,\\
\hat{x}_l^{(k+1)} &= a\hat{x}_{l-1}^{(k)} + \sum_{i=l}^{k-1}\frac{b\hat{x}_i^{(k)}}{c^{i-l+1}}\,, & \hat{y}_l^{(k+1)} &= -b\hat{y}_{l-1}^{(k)} - \sum_{i=l}^{k-1}\frac{(-1)^{i-l}a\hat{y}_i^{(k)}}{c^{i-l+1}}\,,\\
& 1 \le l \le k-1 & & \\
\hat{x}_k^{(k+1)} &= a\hat{x}_{k-1}^{(k)}\,, & \hat{y}_k^{(k+1)} &= -b\hat{y}_{k-1}^{(k)}\,.
\end{aligned} \tag{B.11}$$

Specifically we get $p_0 = q_0 = -\frac{ab}{a-b} = \tilde{x}_0^{(0)} = \tilde{y}_0^{(0)}$. The entire solution in the time domain before the separation of the impacting mass finally results as

$$\begin{aligned}
{}^{(\mathrm{a})}u(\delta,\tilde{t})_{\mathrm{b.s.}} = \alpha t_0\Bigg[&-\tilde{\kappa}v_{\mathrm{m}}\big(h(\tilde{t}-\delta) + h(\tilde{t}+\delta)\big) + gt_0\int_0^{\tilde{t}}(\tilde{t}-\tau)\big(h(\tilde{t}-\delta) - h(\tilde{t}+\delta)\big)\,\mathrm{d}\tau\\
&+ (v_{\mathrm{m}} - g\tilde{\kappa}t_0)\int_0^{\tilde{t}}h(\tau-\delta)\,\mathrm{d}\tau \;-\; (v_{\mathrm{m}} + g\tilde{\kappa}t_0)\int_0^{\tilde{t}}h(\tau+\delta)\,\mathrm{d}\tau\Bigg].
\end{aligned} \tag{B.12}$$

C Assessment of the Separation Time t_{c}

As justification of Eq. (29) it was claimed that the separation condition Eq. (6) comes true at the time $\tilde{t}_{\mathrm{c}} = 2$ respectively $t_{\mathrm{c}} = 2t_0$. This will be confirmed in the following by an explicit discussion of the stress development at the upper end of the rod according to the solution for boundary condition (a) before separation, Eq. (B.12). Following the discussion subsequent to Eq. (23), considering only the first series element, $n = 0$, of the expression Eq. (B.5) already allows for the correct solution representation for $\tilde{t} < 2$. The according stress development at the upper end of the rod, $\delta = 1$, results from Eq. (B.12) as

$${}^{(\mathrm{a})}\sigma_0(1,\tilde{t}) = -\frac{Et_0}{L}\,\mathrm{e}^{-\tilde{t}/\alpha}\left(v_{\mathrm{m}} + \left(\mathrm{e}^{\tilde{t}/\alpha} - 1\right)gt_0\alpha\right) < 0\,, \tag{C.1}$$

providing for the limit from below, $\tilde{t} \to 2^-$,

$${}^{(\mathrm{a})}\sigma_0(1,\tilde{t}\to 2^-) = -\frac{Et_0}{L}\,\mathrm{e}^{-2/\alpha}\left(v_{\mathrm{m}} + \left(\mathrm{e}^{2/\alpha} - 1\right)gt_0\alpha\right). \tag{C.2}$$

Considering the first two series elements, $n = 0, 1$, of the expression Eq. (B.5) for the stress development at the upper end of the rod, $\delta = 1$, gives then the correct solution for $\tilde{t} < 4$. Considering the limit from above, $\tilde{t} \to 2^+$, yields

$$\left[{}^{(\mathrm{a})}\sigma_0 + {}^{(\mathrm{a})}\sigma_1\right](1,\tilde{t}\to 2^+) = -\frac{Et_0}{L}\,\mathrm{e}^{-2/\alpha}\left(-2\mathrm{e}^{2/\alpha}v_{\mathrm{m}} + v_{\mathrm{m}} + \left(\mathrm{e}^{2/\alpha} - 1\right)gt_0\alpha\right). \tag{C.3}$$

Note that at times $\tilde{t} < 2$ (including the limit consideration) effects due to the spring mounting have not yet arrived at the upper end of the rod, therefore the parameter $\tilde{\kappa}$ does not appear here.

Examining the difference of both limits, one finds a step in the stress development at $\tilde{t} = 2$ of magnitude $2Et_0v_\mathrm{m}/L$. This step results in a tensile stress at $\tilde{t} \to 2^+$ when the following condition for the compressive stress holds

$$^{(\mathrm{a})}\sigma_0(1, \tilde{t} \to 2^-) > -\frac{2Et_0}{L}v_\mathrm{m} = -\frac{2E}{c_0}v_\mathrm{m} = -2\bar{\sigma}\,, \tag{C.4}$$

where $\bar{\sigma} = Ev_\mathrm{m}/c_0$ is the maximum absolute stress in the rod for a stiff barrier ($\tilde{\kappa} \to 0$). Actually, the spring allows the lower end of the rod to behave like a free end in the first moment when the stress wave arrives: the total stress of magnitude $\bar{\sigma}$ is mirrored, thus resulting at its upper end at $\tilde{t} = 2^+$ in a step in the stress of magnitude $2\bar{\sigma}$. This is an artefact of the spring, which in this respect is not well representing a compliant bedding of the rod. However, this artefact causes the separation time to be $\tilde{t}_\mathrm{c} = 2$. Only in the limit case, $\tilde{\kappa} \to 0$, compare Sec. 5, the step is no longer resolved, and times for the duration of contact as in Hu and Eberhard (2001) can be determined. From Eq. (C.4) we find the relation for the system parameters

$$gt_0\alpha\left(1 - \mathrm{e}^{-2/\alpha}\right) < v_\mathrm{m}\left(2 - \mathrm{e}^{-2/\alpha}\right)\,, \tag{C.5}$$

which is true for technically relevant cases with typical values $g \sim 10\,\mathrm{m/s^2}$, $\alpha \sim 10$, $t_0 < 2 \cdot 10^{-3}\,\mathrm{s}$, $v_\mathrm{m} \sim 1 - 10\,\mathrm{m/s}$. In order to give a more tangible criterion, the limit case $\alpha \to \infty$ is considered. According to the definition, $\alpha = \frac{m}{\rho AL}$, this represents either the case of an extremely large value of m, the mass of the impacting body, or of a small density ρ of the rod, which then goes along with a high wave propagation speed c_0 in the rod material. Using the Taylor series expansion $\mathrm{e}^{-\tilde{t}/\alpha} \sim 1 - \frac{\tilde{t}}{\alpha} + \mathcal{O}\left(\frac{\tilde{t}^2}{\alpha^2}\right)$, we find from Eq. (C.1)

$$\lim_{\alpha\to\infty} {}^{(\mathrm{a})}\sigma_0(1, \tilde{t}) = -\frac{Et_0}{L}(gt_0\tilde{t} + v_\mathrm{m}) < 0\,, \tag{C.6}$$

which in the limit $\tilde{t} \to 2^-$ fulfills Eq. (C.4) only when $2gt_0 < v_\mathrm{m}$. A minimum impact velocity v_m is thus required to facilitate a separation of the impacting mass from the rod according to the condition (6). The limiting velocity $2gt_0$ originates from elementary model assumptions, namely that we take into account the influence of gravity on the impacting mass only, Eq. (4), but not on the rod, Eq. (1). Entirely neglecting gravity in the model would end up in the trivial condition $0 < v_\mathrm{m}$.

Acknowledgement

The authors would like to express their gratitude to Prof. F. D. Fischer (Institute of Mechanics, Montanuniversität Leoben) and Dr. C. Krempaszky (Christian Doppler Laboratory of Material Mechanics of High Performance Alloys, Technische Universität München) who contributed valuable suggestions to the work.

References

Alterman, Z.; Karal, F. C.: Propagation of elastic waves in a semi-infinite cylindrical rod using finite difference methods. *Journal of Sound and Vibration*, 13, (1970), 115–145.

Boström, A.: On wave equations for elastic rods. *Z. angew. Math. Mech. (ZAMM)*, 80, 4, (2000), 245–251.

Danzer, R.; Fischer, F. D.; Yan, W. Y.: Application of probabilistic fracture mechanics to a dynamic loading situation using the example of a dynamic tension test for ceramics. *Journal of the European Ceramic Society*, 20, (2000), 901–911.

Doetsch, G.: *Introduction to the theory and application of the Laplace transformation*. Springer-Verlag (1974).

Hu, B.; Eberhard, P.: Symbolic computation of longitudinal impact waves. *Computer Methods in Applied Mechanics and Engineering*, 190, 37-38, (2001), 4805-4815.

Matuk, C.: Impact of a linearly elastic rod on a thin linearly viscoelastic target. *Journal of Sound and Vibration*, 64, 1, (1979), 45–55.

Schwarz, C.; Fischer, F. D.; Werner, E.; Dirschmid, H. J.: Impact of an elastic rod on a deformable barrier: analytical and numerical investigations on models of a valve and a rod-shaped stamping tool. *Archive of Applied Mechanics*, 80, 1, (2010a), 3–24.

Schwarz, C.; Werner, E.; Dirschmid, H. J.: 1D wave propagation in a rod: analytic treatment for non-trivial boundary conditions. vol. 10 of *Proceedings in Applied Mathematics and Mechanics*, pages 525–526, Wiley-VCH (2010b).

Shi, P.: Simulation of impact involving an elastic rod. *Computer Methods in Applied Mechanics and Engineering*, 151, (1998a), 497–499.

Shi, P.: The restitution coefficient for a linear elastic rod. *Mathematical and Computer Modelling*, 28, 4-8, (1998b), 427–435.

Skalak, R.: Longitudinal impact of a semi-infinite circular elastic bar. *ASME Journal of Applied Mechanics*, 24, (1957), 59–64.

Sundararajan, G.; Tirupataiah, Y.: The localization of plastic flow under dynamic indentation conditions: I. Experimental results. *Acta Materialia*, 54, 3, (2006), 565–575.

The MathWorks, I.: *Matlab, R2010b*. Natick, Massachusetts (2010).

Valeš, F.; Š. Morávka; Brepta, R.; Červ, J.: Wave propagation in a thick cylindrical bar due to longitudinal impact. *JSME International Journal Series A*, 39, (1996), 60–70.

Werner, E. A.; Fischer, F. D.: The stress state in a moving rod suddenly elastically fixed at its trailing end. *Acta Mechanica*, 111, (1995), 171–179.

Wolfram Research, I.: *Mathematica, Version 7.0*. Champaign, Illinois (2008).

YuFeng, X.; DeChao, Z.: Analytical solutions of impact problems of rod structures with springs. *Computer Methods in Applied Mechanics and Engineering*, 160, 3-4, (1998), 315–323.

Zharkova, N. V.; Nikitin, L. V.: Applied problems in the dynamics of elastic rods. *Mechanics of Solids*, 41, 6, (2006), 64–79.

Addresses: Dr.-Ing. Cornelia Schwarz, Institute of Materials Science and Mechanics of Materials,
Technische Universität München, Boltzmannstr. 15, 85748 Garching, Germany
email: schwarz@wkm.mw.tum.de
Prof. Dr. mont. habil. Dr. h. c. Ewald Werner, Institute of Materials Science and Mechanics of Materials,
Technische Universität München, Boltzmannstr. 15, 85748 Garching, Germany
Prof. Dr. Hans Jörg Dirschmid, Institute of Analysis and Scientific Computing, Technische Universität Wien,
Wiedner Hauptstr. 8, 1040 Vienna, Austria